

Bit Error Rate Analysis of Physical Layer Network Coding Spatially Modulated Full-Duplex Nodes Based Bidirectional Wireless Relay Network

¹R. Rajesh, ²A. Bagubali, ³K. Sasikumar

School of Electronics Engineering
Vellore Institute of Technology
Vellore, India.

¹rajesh@vit.ac.in, ²bagubali@vit.ac.in, ³sasikumar.k@vit.ac.in

Abstract— In this paper, Physical Layer Network coding (PLNC)-Spatially Modulated Full-Duplex (SMFD) nodes based two-way/bidirectional cooperative wireless relay network is proposed. The PLNC-SMFD-based system is a viable technology in the field of next-generation wireless networks to enhance spectral efficiency. In the proposed system model, both the source nodes and relay nodes are employed with 2×2 antenna configurations where 2 bits of information are exchanged between the source nodes through a relay node. Transmit antenna selection at the source nodes is based on the incoming bitstreams. For instance, the transmit antenna is selected at PLNC-SMFD nodes based on the data symbols of the Most Significant Bit (MSB). Whereas the selected transmit antenna sends the Least Significant Bit (LSB) bit of data symbol at any time instance. Further, the self-interference at the transmitting and receiving nodes is modeled as Gaussian with the thermal noise power as a variance. The Bit Error Rate (BER) analytical expressions for both the upper and lower bound are derived in a Rayleigh Fading channel background. It has been graphically shown that the BER performance of the proposed system analyzes the effect of self-interference.

Keywords- physical-layer network coding; spatial modulation; full-duplex; Bit error rate; transmit antenna selection.

I. INTRODUCTION

Spatial-modulation (SM) is a type of multiple-input and multiple-output (MIMO) system. It is a viable technology intensively researched in the wireless communication area because of its capability to enhance Spectral Efficiency (SE), capacity, coverage extension, and data rate [1,2]. SM is a unique combination of digital modulation, coding, and multiple antenna transmission that takes advantage of the wireless channel's location-specific characteristics for communication.

The sparse characteristics of SM aim at designing low complexity modulation schemes and MIMO transceiver architecture for fading channels without deteriorating the spectral efficiency, and data rates respectively [3]. It can overcome the Inter-Channel Interference (ICI) effect and synchronization problems, which is attained by enabling the data to be sent via a single transmit antenna at any time. Therefore, SM completely avoids ICI, transmit antenna synchronization, and multiple RF chain requirements for data transmission [4, 5]. SM could be used in combination with terahertz communications distributed antenna systems, and visible light communications owing to its inherent

advantages [6-8]. The spectral efficiency of systems such as the internet of things can be improved by the use of SM and FD making SMFD systems a prominent issue in recent years [9].

II. RELATED WORKS

The performance of the Bit Error Rate (BER) of a MIMO system with an FD-SM relay is analyzed in [10]. Further, [11], suggests that the bi-directional FD wireless relay channel's source and relay nodes were both subjected to SM, resulting in low-cost high-frequency bi-directional communications. Though there are many advantages of combing the concept of SM and FD, the performance of the systems is majorly affected by residual self-interference. Transmit Antenna Selection (TAS) techniques in [12, 13] have been used to eliminate the self-interference effect. Conversely, self-interference cancellation (SIC) approaches may considerably minimize the effect of self-interference [14]. Recent research studies have shown the effect of self-interference in FD which can be removed up to 110 dB [15, 16].

Cooperative communication networks have lately sparked significant attention in the field of wireless systems,

owing to their prospective benefits of high data throughput and spectrum efficiency [17]. In the traditional wireless HD relay system based on PLNC, the source nodes from both ends broadcast data to a relay node in the occurrence of the first time slot over a Multiple Access Channel (MAC). The relay transmits the encoded signal to both source nodes through a Broadcast Channel (BC) in the second time slot [18]. As a result of the increased time slot needs to convey information between source and relay nodes, traditional half-duplex systems suffer immensely from low spectrum utilization. Whereas in the bidirectional full-duplex wireless system, the merits of PLNC increase spectral efficiency, and capacity, and theoretically double the data rate. Furthermore, to improve spectrum efficiency, the notion of PLNC is used in an FD spatially modulated nodes wireless relay system, which allows transmission nodes to transmit and receive at a single time and frequency slot compared to traditional relay protocols.

The performance of SM and FD under the influence of self-interference has been investigated by deriving analytical equations for Symbol Error Rate, outage probability, and capacity [19]. In [20-23], the performance of FD has been evaluated using the Bit Error Rate (BER), ergodic capacity, and probability of Outage Performance (OP). At high SNR, the BER and OP of FD systems would approach an error floor that cannot be reduced further. Moreover, a lot of work has also been carried out by combining the SM and FD systems. The combination of the SMFD and PLNC techniques in wireless relay networks is now intelligent, and this system may be used in future next-generation wireless networks and beyond [24-26]. But, theoretically, there is always a scope for improving the utilization of spectral efficiency by combining the technology. Inspired by these proofs, this paper drives the limits of bidirectional full-duplex spatial modulation relaying networks by employing the concept of PLNC in SMFD relaying networks. The PLNC-SMFD nodes-based wireless relaying upper and lower bound error performance is analyzed.

The following is a summary of the paper's main contribution:

- The main contribution of this paper is to analyze the BER performance of the PLNC-SMFD-based bidirectional FD wireless relay system. The proposed system model combines the advantage of employing PLNC and SMFD concepts at source nodes and the relay node to enhance spectral efficiency.
- For the proposed system model, the expressions for Signal-to-Interference-plus-Noise-Ratio (SINR)

at the source nodes and the relay node are derived over the Rayleigh fading channel.

- The BER of closed-form analytical formulas is obtained for the end-to-end upper and lower bounds. Moreover, the graphical results illustrate the proposed system's performance with and without the effect of self-interference based on the numerical results derived.

The remainder of this paper is organized as follows. The PLNC-SMFD-based system model is presented in section III. Mathematical expressions are obtained for SINR and BER tight upper bound and lower bound in section IV. Section V describes numerical findings and discussions. Section VI presents the paper's conclusion.

III. SYSTEM MODEL

The system model proposed for the PLNC-SMFD nodes-based bidirectional wireless relay system consists of two source nodes S_1, S_2 and a relay node R as shown in Figure 1.

In the proposed system model, both the source nodes and relay nodes are employed with 2×2 antenna configurations where all the nodes operate in PLNC-SMFD mode. Based on the incoming bitstream, the transmitter selects one transmits antenna and the other act as the receiver antenna. Assume that there is a shadowing effect because of no line-of-sight communication between the PLNC-SMFD source nodes. The PLNC-SMFD source nodes S_1 & S_2 exchange 2 bits of the information bitstream of data symbol $x_k \in \{1, 2\}$ through the relay node R . Transmit antenna is selected at PLNC-SMFD source nodes based on the data symbols of Most Significant Bit (MSB). The selection of transmit antenna at the k^{th} source

node $S_k, k = 1, 2$ is given by
$$j_k = \begin{cases} 1 & \text{if } b_k^{MSB}[n] = 1 \\ 0 & \text{if } b_k^{MSB}[n] = 0 \end{cases}$$

BPSK data symbol $x_k^{LSB}[n] = 2b_k^{LSB}[n] - 1, k = 1, 2$ is transmitted simultaneously by both the PLNC-SMFD source nodes of the selected transmit antenna to the SMFD relay node R .

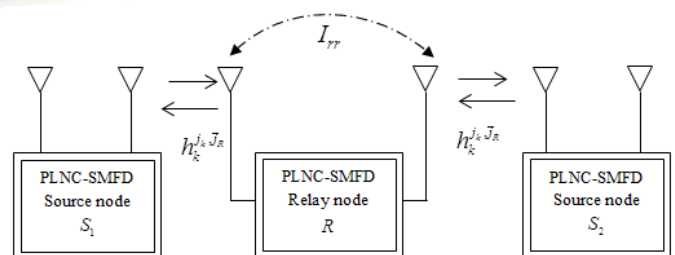


Figure 1. PLNC-SMFD nodes-based bidirectional wireless relay system model

The PLNC-SMFD-based relay node R received signal in n^{th} the time slot given by

$$y_{r'}^{\bar{j}_r}[n] = \sum_{k=1}^2 \sqrt{E_k} h_k^{j_k, \bar{j}_r} x_k^{LSB}[n] + I_{rr}[n] + w_r[n] \quad k=1, 2 \quad (1)$$

Let $h_k^{j_k, \bar{j}_r}, k=1,2$ denotes the PLNC-SMFD k^{th} source node selected transmit antenna j_k and the relay node R receive antenna \bar{j}_r impulse response of the channel. $E_k, k=1,2$ denotes the transmit power of PLNC-SMFD source nodes $S_k, k=1,2$. At the relay node R , the self-interference I_{rr} is Gaussian modeled with the zero mean and variance expressed in terms of thermal noise power $I_r = N_0 \left[10^{\frac{\beta}{10}} - 1 \right] \beta \geq 0$ [28]

$w_r[n]$ is Additive White Gaussian Noise (AWGN) model distribution. Assuming at the PLNC-SMFD relay node R , the information about the Channel Status is known. Based on the Maximum Likelihood (ML) detection method $j_1, j_2, x_1^{LSB}[n], x_2^{LSB}[n]$ parameters are detected as given by

$$\left(\hat{j}_1, \hat{j}_2, \hat{x}_1^{LSB}[n], \hat{x}_2^{LSB}[n] \right) = \left\{ \min_{\substack{j_1, j_2, x_1^{LSB}[n], x_2^{LSB}[n]}} \left| y_{r'}^{\bar{j}_r}[n] - \sum_{k=1}^2 \sqrt{E_k} h_k^{j_k, \bar{j}_r} x_k^{LSB}[n] \right|^2 \right\} k=1, 2 \quad (2)$$

The selection of transmit antenna at the PLNC-SMFD relay node R is $j_r = \hat{j}_1 \oplus \hat{j}_2$. The PLNC-SMFD relay node R then transmits the detected symbol $x_r^{LSB}[n] = \hat{x}_1^{LSB}[n] \oplus \hat{x}_2^{LSB}[n]$ to the source nodes $S_k, k=1, 2$ The signal received at PLNC-SMFD source nodes $S_k, k=1, 2$ is given by

$$y_k^{\bar{j}_k} = \sqrt{E_r} h_k^{\bar{j}_k, j_r} x_r^{LSB}[n] + i_{kk}[n] + w_k[n], \quad k=1, 2 \quad (3)$$

Using the ML method, the parameters $j_r, x_r[n]$ are estimated as

$$\left(\hat{j}_r, \hat{x}_r^{LSB}[n] \right) = \min_{j_r, x_r^{LSB}[n]} \left| y_k^{\bar{j}_k}[n] - \sqrt{E_r} h_k^{\bar{j}_k, j_r} x_r^{LSB}[n] \right|^2 \quad (4)$$

The estimated data symbols at the terminals of the k^{th} source node $S_k, k=1, 2$ can be written as

$$\hat{x}_k^{MSB}[n] = \hat{j}_r \oplus j_k \quad k=1, 2 \quad (5)$$

$$\hat{x}_k^{LSB}[n] = \hat{x}_r^{LSB}[n] \oplus x_k^{LSB}[n] \quad k=1, 2 \quad (6)$$

IV. BIT ERROR RATE PERFORMANCE ANALYSIS

The performance of BER has been derived analytically in a rayleigh fading background for the upper bound and lower bound of the PLNC-SMFD nodes based bidirectional wireless relay system proposed.

A. End-to-End Upper Bound Error Probability

Let $SNR_k = E_k/N_0, k=1, 2, SNR_R = E_r/N_0$ be the source node and relay node SNR respectively. The SINR of PLNC-SMFD source node $S_k, k=1, 2$ and the relay node R is expressed as

$$\gamma_{S_k, R}^{\bar{j}_r} = \frac{SNR_k \left| h_k^{j_k, \bar{j}_r} \right|^2}{(I_r/N_0) + 1} \quad k=1, 2 \quad (7)$$

Using equation (3), Due to PLNC-SMFD relay node R , the source node $S_k, k=1, 2$ SINR is expressed as

$$\gamma_{R, S_k}^{\bar{j}_k} = \frac{SNR_R \left| h_k^{\bar{j}_k, j_r} \right|^2}{(I_r/N_0) + 1} \quad k=1, 2 \quad (8)$$

The upper and lower bound probability of the proposed PLNC-SMFD nodes wireless relay is expressed as

$$P_e^{UB-R} = \frac{1}{2} \left(Q \left(\sqrt{2\gamma_{S_1^0, R}} \right) + Q \left(\sqrt{2\gamma_{S_1^1, R}} \right) \right) + \frac{1}{2} \left(Q \left(\sqrt{2\gamma_{S_2^0, R}} \right) + Q \left(\sqrt{2\gamma_{S_2^1, R}} \right) \right) \quad (9)$$

$$P_e^{LB-R} = Q \left(\sqrt{\min \left(\gamma_{S_1^0, R}, \gamma_{S_1^1, R}, \gamma_{S_2^0, R}, \gamma_{S_2^1, R} \right)} \right) \quad (10)$$

The error probability for the upper bound at the source node $S_k, k=1, 2$ due to the relay node R being expressed as

$$P_e^{UB-R} = \int_0^\infty \frac{1}{2} Q \left(\sqrt{2\gamma_{S_1^0, R}} \right) f_{\gamma_{S_1^0, R}} \left(\gamma_{S_1^0, R} \right) d\gamma_{S_1^0, R} + \frac{1}{2} \int_0^\infty Q \left(\sqrt{2\gamma_{S_1^1, R}} \right) f_{\gamma_{S_1^1, R}} \left(\gamma_{S_1^1, R} \right) d\gamma_{S_1^1, R} + \int_0^\infty \frac{1}{2} Q \left(\sqrt{2\gamma_{S_2^0, R}} \right) f_{\gamma_{S_2^0, R}} \left(\gamma_{S_2^0, R} \right) d\gamma_{S_2^0, R} + \frac{1}{2} \int_0^\infty Q \left(\sqrt{2\gamma_{S_2^1, R}} \right) f_{\gamma_{S_2^1, R}} \left(\gamma_{S_2^1, R} \right) d\gamma_{S_2^1, R} \quad (11)$$

Let $X_{k, j_k, \bar{j}_r} = \left| h_k^{j_k, \bar{j}_r} \right|^2$ follows an exponential distribution with zero mean and variance $\sigma_{k, j_k, \bar{j}_r}^2, \bar{j}_r = 0, 1$. The Cumulative

Distribution Function (CDF) $\gamma_{S_k, R}^{\bar{j}_r}$ is expressed by using [27]

as

$$F_{\gamma_{S_k,R}^{\bar{J}_r}} = \left[1 - \exp\left(-\frac{2((I_r/N_0)+1)}{SNR_k \sigma_{k,\bar{J}_k,\bar{J}_r}^2}\right) \right]^{\bar{J}_r}, \bar{J}_r = 0,1 \text{ and } k = 1,2 \quad (12)$$

Using the CDF in equation (12), the Probability Density Function (PDF) is obtained by

$$f_{\gamma_{S_k,R}^{\bar{J}_r}}(\gamma_{S_k,R}^{\bar{J}_r}) = \frac{dF_{\gamma_{S_k,R}^{\bar{J}_r}}}{d\gamma_{S_k,R}^{\bar{J}_r}}, \bar{J}_r = 0,1 \text{ and } k = 1,2 \quad (13)$$

Substituting equation (12) in equation (13), the PDF $f_{\gamma_{S_k,R}^{\bar{J}_r}}(\gamma_{S_k,R}^{\bar{J}_r})$, $\bar{J}_r = 0,1$ and $k = 1,2$ can be written as

$$f_{\gamma_{S_k,R}^{\bar{J}_r}}(\gamma_{S_k,R}^{\bar{J}_r}) = \left\{ \frac{2((I_r/N_0)+1)}{SNR_k \sigma_{k,\bar{J}_k,\bar{J}_r}^2} e^{-\frac{2((I_r/N_0)+1)\gamma_{S_k,R}^{\bar{J}_r}}{SNR_k \sigma_{k,\bar{J}_k,\bar{J}_r}^2}} \right\} \quad (14)$$

Using Q function property [29], \tilde{P}_e^{UB-R} for $\gamma_{S_k,R}^{\bar{J}_r}$, $\bar{J}_r = 0,1$ and $k = 1,2$ can be written as

$$P_e^{UB-R} = \int_0^\infty \frac{1}{2} Q\left(\sqrt{2\gamma_{S_k,R}^{\bar{J}_r}}\right) f_{\gamma_{S_k,R}^{\bar{J}_r}}(\gamma_{S_k,R}^{\bar{J}_r}) d\gamma_{S_k,R}^{\bar{J}_r} \quad (15)$$

By substituting, equation (14) and equation (15) in equation (11), the PDF of $f_{\gamma_{S_k,R}^{\bar{J}_r}}(\gamma_{S_k,R}^{\bar{J}_r})$, $\bar{J}_r = 0,1$ and $k = 1,2$ and after simple calculations is computed as

$$P_e^{UB-R} = \left(1 - \sqrt{\frac{SNR_k \sigma_{k,\bar{J}_k,\bar{J}_r}^2}{2(I_r/N_0 + 1) + SNR_k \sigma_{k,\bar{J}_k,\bar{J}_r}^2}} \right) \quad (16)$$

Similarly, the upper bound error performance at the PLNC-SMFD source nodes $S_k, k = 1,2$ can be expressed as

$$P_e^{S_k} = \frac{1}{2} \left(Q\sqrt{2\gamma_{R^0,S_k}} + Q\sqrt{2\gamma_{R^1,S_k}} \right) \quad k = 1, 2 \quad (17)$$

The error probability at the source $S_k, k = 1,2$ using the Q function [29] can be expressed as

$$P_e^{S_k} = \int_0^\infty \frac{1}{2} Q\left(\sqrt{2\gamma_{R^0,S_1}}\right) f_{R^0,S_1}(\gamma_{R^0,S_1}) d\gamma_{R^0,S_1} + \frac{1}{2} \int_0^\infty Q\left(\sqrt{2\gamma_{R^1,S_2}}\right) f_{R^1,S_2}(\gamma_{R^1,S_2}) d\gamma_{R^0,S_2} \quad (18)$$

Let $X_{k,\bar{J}_k,\bar{J}_r} = |h_{k,\bar{J}_k,\bar{J}_r}|$ follows an exponential distribution with zero mean and variance $\sigma_{k,\bar{J}_k,\bar{J}_r}^2$, $\bar{J}_k = 0, 1$. The CDF $F_{\gamma_{R,S_k}^{\bar{J}_k}}$ is calculated as

$$F_{\gamma_{R,S_k}^{\bar{J}_k}} = \left[1 - \exp\left(-\frac{2((I_r/N_0)+1)}{SNR_R \sigma_{k,\bar{J}_k,\bar{J}_r}^2}\right) \right]^{\bar{J}_k}, \bar{J}_k = 0,1 \text{ and } k = 1,2 \quad (19)$$

Using CDF in equation (19), the PDF $f_{\gamma_{R,S_k}^{\bar{J}_k}}$ obtained by

$$f_{\gamma_{R,S_k}^{\bar{J}_k}}(\gamma_{R,S_k}^{\bar{J}_k}) = \frac{dF_{\gamma_{R,S_k}^{\bar{J}_k}}}{d\gamma_{R,S_k}^{\bar{J}_k}}, \bar{J}_k = 0,1 \text{ and } k = 1,2 \quad (20)$$

Substituting the equation (19) in equation (20), the PDF $f_{\gamma_{R,S_k}^{\bar{J}_k}}(\gamma_{R,S_k}^{\bar{J}_k})$, $\bar{J}_k = 0,1$ and $k = 1,2$ can be written as

$$f_{\gamma_{R,S_k}^{\bar{J}_k}}(\gamma_{R,S_k}^{\bar{J}_k}) = \left(\frac{2((I_r/N_0)+1)}{SNR_R \sigma_{k,\bar{J}_k,\bar{J}_r}^2} \right) e^{-\frac{2((I_r/N_0)+1)\gamma_{R,S_k}^{\bar{J}_k}}{SNR_R \sigma_{k,\bar{J}_k,\bar{J}_r}^2}} \quad (21)$$

Using the Q function property [29], $P_e^{S_k}$ for $\gamma_{R,S_k}^{\bar{J}_k}$, $\bar{J}_k = 0,1$ and $k = 1,2$ can be written as

$$P_e^{S_k} = \int_0^\infty \frac{1}{2} Q\left(\sqrt{2\gamma_{R,S_k}^{\bar{J}_k}}\right) f_{\gamma_{R,S_k}^{\bar{J}_k}}(\gamma_{R,S_k}^{\bar{J}_k}) d\gamma_{R,S_k}^{\bar{J}_k} \quad (22)$$

By substituting equation (21) in equation (22) and by using PDF of $f_{\gamma_{R,S_k}^{\bar{J}_k}}(\gamma_{R,S_k}^{\bar{J}_k})$, $\bar{J}_k = 0,1$ and $k = 1,2$, the upper bound error probability after rigorous calculations is computed as

$$P_e^{S_k} = \frac{1}{2} \prod_{\bar{J}_k=0}^1 \left(1 - \sqrt{\frac{SNR_R \sigma_{k,\bar{J}_k,\bar{J}_r}^2}{2(I_r/N_0 + 1) + SNR_R \sigma_{k,\bar{J}_k,\bar{J}_r}^2}} \right) \quad k = 1,2 \quad (23)$$

The probability of error performance for the overall upper bound is obtained by merging the error performance at the source nodes $S_k, k = 1,2$ and the relay node R . It is defined as

$$\tilde{P}_e^{PLNC-SMFD(UB)} = P_e^{UB-R} + (1 - P_e^{UB-R}) P_e^{S_k} \quad (24)$$

Substituting equation (16) and equation (23) in equation (24), the error performance probability for the entire upper bound is represented as

$$P_e^{UB} = \left\{ \left(1 - \sqrt{\frac{SNR_k \sigma_{k,\bar{J}_k,\bar{J}_r}^2}{2\left(\frac{I_r}{N_0} + 1\right) + SNR_k \sigma_{k,\bar{J}_k,\bar{J}_r}^2}} \right) + \left(\sqrt{\frac{SNR_k \sigma_{k,\bar{J}_k,\bar{J}_r}^2}{2\left(\frac{I_r}{N_0} + 1\right) + SNR_k \sigma_{k,\bar{J}_k,\bar{J}_r}^2}} \right) \right\} \times \prod_{\bar{J}_k=0}^1 \frac{1}{2} \left(1 - \sqrt{\frac{SNR_R \sigma_{k,\bar{J}_k,\bar{J}_r}^2}{2\left(\frac{I_r}{N_0} + 1\right) + SNR_R \sigma_{k,\bar{J}_k,\bar{J}_r}^2}} \right) \quad (25)$$

$$\begin{aligned} \tilde{P}_e^{PLNC-SMFD(LB)} = & 1 - \prod_{k=1}^2 \frac{1}{2} \left[\left(1 - \sqrt{\frac{SNR_k \sigma_{k,j_k,0}^2}{4 \left(\frac{I_r}{N_0} + 1 \right) + SNR_R \sigma_{k,j_k,0}^2}} \right) + \left(1 - \sqrt{\frac{SNR_k \sigma_{k,j_k,1}^2}{4 \left(\frac{I_r}{N_0} + 1 \right) + SNR_R \sigma_{k,j_k,1}^2}} \right) \right] \\ & + \left(\prod_{k=1}^2 \frac{1}{2} \left[\left(1 - \sqrt{\frac{SNR_k \sigma_{k,j_k,0}^2}{4 \left(\frac{I_r}{N_0} + 1 \right) + SNR_R \sigma_{k,j_k,0}^2}} \right) + \left(1 - \sqrt{\frac{SNR_k \sigma_{k,j_k,1}^2}{4 \left(\frac{I_r}{N_0} + 1 \right) + SNR_R \sigma_{k,j_k,1}^2}} \right) \right] \right) \\ & \times \left(\prod_{\bar{j}_k=0}^1 \frac{1}{2} \left(1 - \sqrt{\frac{SNR_k \sigma_{k,j_k,\bar{j}_R}^2}{2 \left(\frac{I_r}{N_0} + 1 \right) SNR_k \sigma_{k,j_k,\bar{j}_R}^2}} \right) \right) \end{aligned} \quad (29)$$

B. End-to-End Lower Bound Error Probability

The probability of error due to the lower bound at the PLNC-SMFD relay node R is given by

$$P_e^{LB-R} = Q \left(\sqrt{2 \min(\gamma_{S_1,R}^0, \gamma_{S_1,R}^1, \gamma_{S_2,R}^0, \gamma_{S_2,R}^1)} \right) \quad (26)$$

The probability of error due to the lower bound based on the data communication between the relay node R and source nodes $S_k, k = 1, 2$ is evaluated as

$$P_e^{LB-R} = 1 - \prod_{k=1}^2 \frac{1}{2} \left[\left(1 - \sqrt{\frac{SNR_k \sigma_{k,j_k,0}^2}{4 \left(\frac{I_r}{N_0} + 1 \right) + SNR_k \sigma_{k,j_k,0}^2}} \right) + \left(1 - \sqrt{\frac{SNR_k \sigma_{k,j_k,1}^2}{4 \left(\frac{I_r}{N_0} + 1 \right) + SNR_k \sigma_{k,j_k,1}^2}} \right) \right] \quad (27)$$

The probability of lower bound overall error is defined as

$$\tilde{P}_e^{PLNC-SMFD(LB)} = P_e^{LB-R} + (1 - P_e^{LB-R}) P_e^{S_k} \quad (28)$$

Substituting equation (23) and equation (27) in equation (28), the probability of lower bound overall error expression is expressed in equation (29).

V. NUMERICAL RESULTS

Based on the analytical expressions derived, In this section, graphical results and discussions are presented and analyzed for the end-to-end upper and lower error performance of PLNC-SMFD nodes-based wireless relay system. The list of parameters and the values are listed in Table 1.

TABLE I. PARAMETERS LIST

S. No	List of parameters	Values
1.	SNR loss Factor (β)	0, 3 dB
2.	Source nodes Signal-to-noise ratio (SNR_k), $k = 1, 2$	0-40 dB
3.	Signal-to-noise ratio at the relay node (SNR_R)	0-40 dB

Fig. 2 shows the upper bound and lower bound overall BER performance of the proposed PLNC-SMFD nodes-based wireless system for the SNR loss factor of $\beta = 0$ dB and $SNR_R = 5, 10, \text{ and } 20$ dB respectively. It has been observed that the increase in the value of SNR at the relay node R reduces the error rate of the proposed system at both the lower and upper bound. Further, it has been noticed, that there are differences in BER performance between upper and lower bounds at the lower range of SNR values ranges 0–15 dB. Moreover, Further, increase in SNR values greater than 15 dB, the error floor is the same for the upper and lower bound. Analytical expressions derived are validated using Monte Carlo simulation.

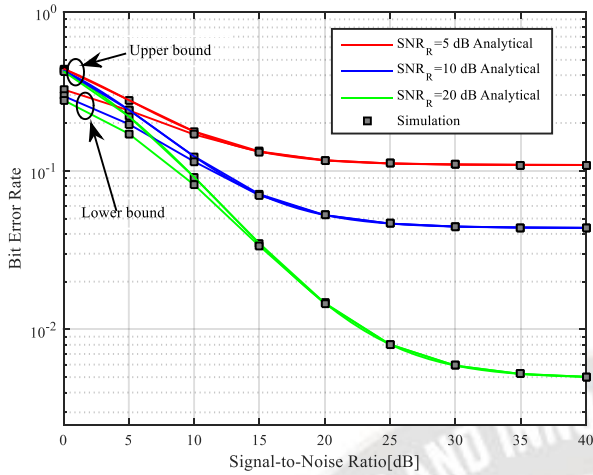


Figure 2. BER of the proposed PLNC-SMFD nodes wireless relay system in Rayleigh fading channel without self-interference factor $\beta=0$.

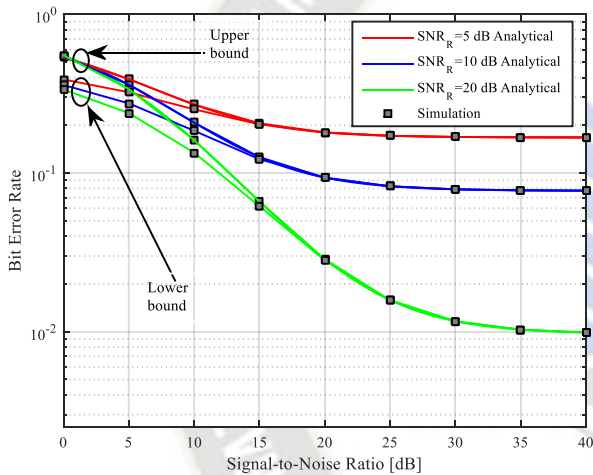


Figure 3. BER of the proposed PLNC-SMFD nodes wireless relay system in Rayleigh fading with self-interference factor $\beta=3$.

Fig. 3 illustrates the upper bound and lower bound overall BER performance of the proposed PLNC-SMFD nodes-based wireless system by considering the effect of self-interference at both the source and relay nodes. The self-interference is modeled as thermal noise power $I_r/N_0 = [10^{\beta/10} - 1]$ $\beta \geq 0$ for the SNR loss factor of $\beta=3$, SNR at the relay nodes R ranges $SNR_R=5, 10$, and 20 dB respectively. It has been witnessed that there is an error rate in the system increases due to the increase in the effect of self-interference compared to the error performance $\beta=0$. In addition to the self-interference impact, the differences in error performances are small at the lower range of SNR values $0-15$ dB. Further, at high SNR values of greater than 15 dB, the error floor saturates and the same for the upper and lower bound.

In Figure 4, the BER of the proposed PLNC-SMFD node is analyzed by considering the constant SNR values at both the source nodes $SNR_k=0-30$ dB $k=1, 2$, relay node $SNR_R=0-30$ dB, and $\beta=0, 3$ dB. It has been observed that the BER performance at 10^{-1} and $\beta=0, 3$ dB, there is a constant 3 dB gap difference in both the upper and lower bound case. For instance, the BER performance 10^{-1} in the case of lower bound error performance at $\beta=0$ dB, the SNR requirement is ~ 10 dB and ~ 13 dB whereas in the case of $\beta=3$ dB the SNR requirement more is ~ 11 dB and ~ 14 dB. It has been observed that an increase in the self-interference effect reduces the error performances.

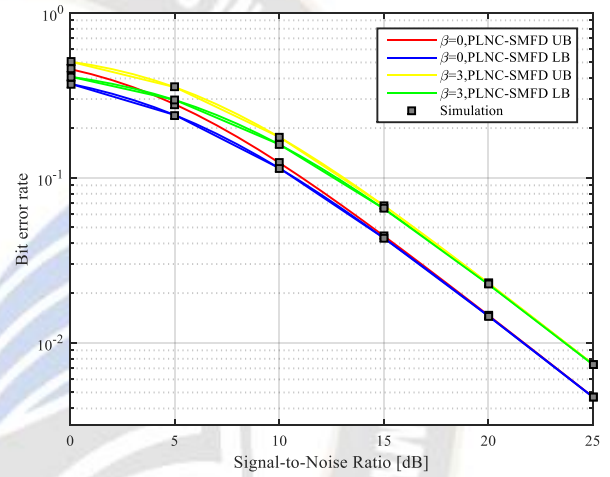


Figure 4. Average BER of the proposed PLNC-SMFD nodes wireless relay system $\beta=0$, and 3 dB.

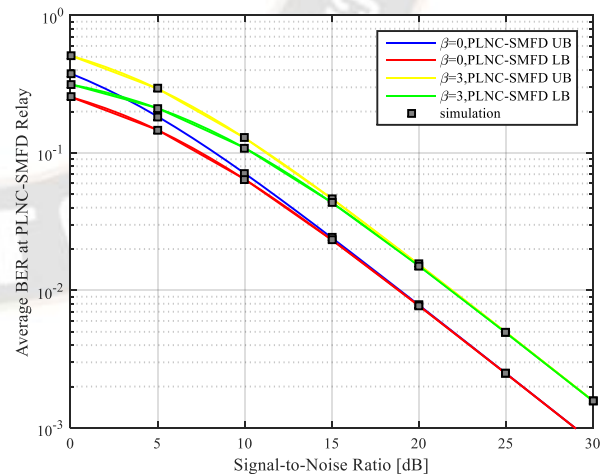


Figure 5. Average BER of PLNC-SMFD nodes wireless Relay node R as $\beta=0$, and 3 dB.

Fig. 5 illustrates the average BER performance at the PLNC-SMFD relay node R, $\beta=0, 3$ dB for upper and lower bounds respectively. For instance, in the lower bound case,

10^{-1} $\beta = 0,3$ dB it has been observed that the SNR requirement is ~ 7 dB and ~ 10 dB whereas in the upper bound the SNR requirement is ~ 8 dB and ~ 11 dB. Further, it has been noticed that increase in the SNR values greater than 15 dB the error bounds are the same.

VI. CONCLUSION

The BER analysis of PLNC-SMFD nodes-based bidirectional wireless relay system is proposed in this paper. The merits of PLNC and SMFD are combined in the proposed wireless relay system to increase the spectral efficiency of the wireless systems. The overall end-to-end upper and lower bound error probability analytical expressions are derived under Rayleigh fading channel conditions. The BER analytical results and discussions have shown and analyzed the impact of self-interference. Monte-Carlo simulations in MATLAB validate the analytical results derived.

REFERENCES

- [1] Si, Qintuya, Minglu Jin, Yunfei Chen, Nan Zhao, and Xianbin Wang. "Performance analysis of spatial modulation aided NOMA with the full-duplex relay." *IEEE Transactions on Vehicular Technology*, vol. 69, no. 5, pp.5683-5687, March 2020.
- [2] Li, Qiang, Miaowen Wen, Ertugrul Basar, H. Vincent Poor, and Fangjiong Chen. "Spatial modulation-aided cooperative NOMA: Performance analysis and comparative study." *IEEE Journal of Selected Topics in Signal Processing*, vol. 13, no. 3, pp. 715-728, Feb 2019.
- [3] Aydin, Erdogan, Fatih Cogen, and Ertugrul Basar. "Code-index modulation aided quadrature spatial modulation for high-rate MIMO systems." *IEEE Transactions on Vehicular Technology*, vol. 68, no. 10, pp.10257-10261.jul. 2019.
- [4] Nguyen, Ba Cao, and Xuan Nam Tran. "On the performance of full-duplex spatial modulation MIMO system with and without transmit antenna selection under imperfect hardware conditions." *IEEE Access* vol. 8, pp. 185218-185231.Oct.,2020.
- [5] Bhowal, Anirban, and Rakesh Singh Kshetrimayum. "Outage probability bound of decode and forward two-way full-duplex relay employing spatial modulation over cascaded α - μ channels." *International Journal of Communication Systems* 32, no. 3, .Feb., 2019.
- [6] Gao, Xiang, Zhiquan Bai, Peng Gong, and Dapeng Oliver Wu. "Design and performance analysis of LED-grouping based spatial modulation in the visible light communication system." *IEEE Transactions on Vehicular Technology*, vol. 69, no. 7, pp.7317-7324.April, 2020.
- [7] Bhowal, Anirban, and Rakesh Singh Kshetrimayum. "Outage probability bound of decode and forward two-way relay employing optical spatial modulation over gamma-gamma channels." *IET Optoelectronics* 13, no. 4,pp.183-190,Aug., 2019.
- [8] Mao, Tianqi, Qi Wang, and Zhaocheng Wang. "Spatial modulation for terahertz communication systems with hardware impairments." *IEEE Transactions on Vehicular Technology* vol.69, no. 4, pp. 4553-4557, Feb. 2020.
- [9] Nguyen, Le Van, Ba Cao Nguyen, Xuan Nam Tran, and Le The Dung. "Closed-form expression for the symbol error probability in full-duplex spatial modulation relay system and its application in optimal power allocation." *Sensors* vol. 19, no. 24, pp. 5390, Dec. 2019.
- [10] Liu, Haoran, Yue Xiao, Ping Yang, Jialiang Fu, Shaoqian Li, and Wei Xiang. "Transmit antenna selection for full-duplex spatial modulation based on machine learning." *IEEE Transactions on Vehicular Technology*, vol.70, no. 10, pp. 10695-10708, Sep., 2021.
- [11] Agarwal, D. A. . (2022). Advancing Privacy and Security of Internet of Things to Find Integrated Solutions. *International Journal on Future Revolution in Computer Science & Communication Engineering*, 8(2), 05–08. <https://doi.org/10.17762/ijfrcsce.v8i2.2067>
- [12] Jiang, Xinyi, Xiaoyu Liu, Riqing Chen, Yuntian Wang, Feng Shu, and Jiangzhou Wang. "Efficient receive beamformers for secure spatial modulation against a malicious full-duplex attacker with eavesdropping ability." *IEEE Transactions on Vehicular Technology*, vol. 70, no. 2, pp. 1962-1966, Jan., 2021.
- [13] Nguyen, Ba Cao, and Xuan Nam Tran. "Performance analysis of full-duplex spatial modulation systems with transmit antenna selection." In *2019 International Conference on Advanced Technologies for Communications (ATCIEEE)*, Oct., 2019, , pp. 282-286.
- [14] Nguyen, Ba Cao, and Xuan Nam Tran. "On the performance of full-duplex spatial modulation MIMO system with and without transmit antenna selection under imperfect hardware conditions." *IEEE Access*, vol. 8, pp. 185218-185231, Oct. 2020.
- [15] Kristensen, Andreas Toftgaard, Andreas Burg, and Alexios Balatsoukas-Stimming. "Advanced machine learning techniques for self-interference cancellation in full-duplex radios." In *2019 53rd Asilomar Conference on Signals, Systems, and Computers*, IEEE, Nov., 2019, pp. 1149-1153.
- [16] Zhou, Yanni, Florin Hutu, and Guillaume Villemaud. "Impact of receiver non-idealities on a full duplex spatial modulation system performance." *IEEE Wireless Communications Letters* vol. 9, no. 12 , pp. 2083-2087, Jul., 2020.
- [17] Nguyen, Ba Cao, and Xuan Nam Tran. "Transmit antenna selection for full-duplex spatial modulation multiple-input multiple-output system." *IEEE Systems Journal*, vol. 14, no. 4, pp. 4777-4785, Jan., 2020.
- [18] Chen, Pingping, Zhaopeng Xie, Yi Fang, Zhifeng Chen, Shahid Mumtaz, and Joel JPC Rodrigues. "Physical-layer network coding: An efficient technique for wireless communications." *IEEE Network* vol., 34, no. 2, pp. 270-276,Oct., 2019.
- [19] Pan, Haoyuan, Tse-Tin Chan, Victor CM Leung, and Jianqiang Li. "Age of Information in Physical-Layer

- Network Coding Enabled Two-Way Relay Networks." *IEEE Transactions on Mobile Computing, Apr., 2022.*
- [20] Gazestani, Amirhosein Hajihoseini, Seyed Ali Ghorashi, Behnaz Mousavinasab, and Mohammad Shikh-Bahaei. "A survey on implementation and applications of full duplex wireless communications." *Physical Communication*, vol. 34 pp. 121-134, Jun., 2019.
- [21] Bhowal, Anirban, and Rakhesh Singh Kshetrimayum. "Relay based hybrid FSO/RF communication with hybrid spatial modulation and transmit source selection." *IEEE Transactions on Communications*, vol.68, no. 8, pp. 5018-5027. April, 2020.
- [22] Linda R. Musser. (2020). Older Engineering Books are Open Educational Resources. *Journal of Online Engineering Education*, 11(2), 08–10. Retrieved from <http://onlineengineeringeducation.com/index.php/joe/article/view/41>
- [23] Ravindran Unnithan Jalaja, Renjith, P. G. S. Velmurugan, and S. J. Thiruvengadam. "Performance Analysis of Energy Efficient Spatial Modulation in Bidirectional Cooperative Cognitive Radio System with Eavesdropper." *Wireless Personal Communications*, pp. 1-18, Jan., 2022.
- [24] Elganimi, Taissir Y., Fatima I. Alwerfly, and Akram A. Marseet. "Distributed generalized spatial modulation for relay networks." In 2020 28th Signal Processing and Communications Applications Conference (SIU), IEEE, Oct., 2020, pp. 1-4.
- [25] Butuner, R., & Calp, M. (2022). Diagnosis and Detection of COVID-19 from Lung Tomography Images Using Deep Learning and Machine Learning Methods. *International Journal of Intelligent Systems and Applications in Engineering*, 10(2), 190–200. Retrieved from <https://ijisae.org/index.php/IJISAE/article/view/1843>
- [26] Hassan, Jamal A., and Samah A. Mustafa. "Capacity of Cooperative Spatial Modulation (CSM) System with Optimum Relay Selection." *Wireless Communications and Mobile Computing* 2020, July, 2020.
- [27] Nguyen, Toan-Van, Van-Dinh Nguyen, Daniel Benevides da Costa, and Beongku An. "Hybrid user pairing for spectral and energy efficiencies in multiuser MISO-NOMA networks with SWIPT." *IEEE Transactions on Communication*, vol. 68, no. 8, pp. 4874-4890, May, 2020.
- [28] Abouhogail, R. A. (2022). Untraceable Authentication Protocol for IEEE802.11s Standard. *International Journal of Communication Networks and Information Security (IJCNIS)*, 13(3).
- [29] Li, Qiang, Miaowen Wen, Bruno Clerckx, Shahid Mumtaz, Anwer Al-Dulaimi, and Rose Qingyang Hu. "Subcarrier index modulation for future wireless networks: Principles, applications, and challenges." *IEEE Wireless Communications*, vol. 27, no. 3, pp. 118-125, April, 2020.
- [30] Han, Yonghee, Bhaskar D. Rao, and Jungwoo Lee. "Massive uncoordinated access with massive MIMO: A dictionary learning approach." *IEEE Transactions on Wireless Communications*, vol. 19, no. 2, pp. 1320-1332. Nov., 2019.
- [31] Rajesh, R., P. G. S. Velmurugan, S. J. Thiruvengadam, and P. S. Mallick. "Outage performance of physical layer network coding based spatially modulated full duplex bidirectional relay network." In 2017 International Conference on Wireless Communications, Signal Processing and Networking (WiSPNET), IEEE, March, 2017, pp. 1946-1950.
- [32] Bhowal, Anirban, and Rakhesh Singh Kshetrimayum. *Advanced Spatial Modulation Systems*. Springer, Jan., 2021.
- [33] Ahmad, M., EL-Emam, N. N., & AL-Azawi, A. F. (2022). Improved Deep Hiding/Extraction Algorithm to Enhance the Payload Capacity and Security Level of Hidden Information. *International Journal of Communication Networks and Information Security (IJCNIS)*, 13(3).
- [34] Bhooshan, Sunil. *Fundamentals of Analogue and Digital Communication Systems*. Springer, 2022.